Thermally Triggerable, Anchoring Block Copolymers for use in Aqueous Inkjet Printing

*George E. Parkes,[1] Helena J. Hutchins-Crawford,[1] Claire Bourdin,[2] Stuart Reynolds,[2] Laura Leslie,[1] Matthew J. Derry,[1] Josephine L Harries,[2] Paul D. Topham[1]**

[1] Aston Institute of Materials Research, Aston University, Aston Triangle, Birmingham, B4 7ET, UK.

[2] Domino Printing UK, Trafalgar Way, Bar Hill, Cambridge, CB23 8TU, UK.

*Corresponding author: p.d.topham@aston.ac.uk

Abstract

Towards the goal of shifting from toxic organic solvents to aqueous-based formulations in commercial inkjet printing, a series of well-defined poly[(2-hydroxyethyl acrylate-*stat*-*N*-hydroxymethyl acrylamide)-*block*-propyl methacrylate], P[(HEA-*st*-HMAA)-*b*-PMA)], amphiphilic block copolymers with varying degrees of polymerization and comonomer compositions were synthesized *via* reversible addition-fragmentation chain transfer (RAFT) polymerization. Optimized RAFT polymerization conditions were found to allow larger batch

synthesis (> 20 g scale) without compromise over molecular design control (molecular mass, hydrophobic/hydrophilic balance, dispersity, etc.). The copolymers were subsequently investigated for their crosslinking and adhesive properties, as well as jetting performance, to determine their suitability for use in aqueous ink formulations. Crosslinking was found to occur much faster for copolymers containing more of the crosslinkable HMAA monomer units and at higher molecular masses, allowing control over the required post-deposition processing time. The amphiphilic block copolymers synthesized herein demonstrate enhanced adhesive properties compared to a selection of commercial inks whilst also achieving high print quality and performance for use in aqueous continuous inkjet (CIJ) printing, which is a key step towards greener processes in the packaging industries, where printing onto hydrophobic substrates is needed.

Introduction

Inkjet printing has been prevalent in households, offices, photography and graphics for decades.[1] Although hardcopy printing has recently declined due to our shift towards a more electronic, "paper-less" society, industrial printing for consumer products (such as food packaging, cosmetics, hygiene products, etc.) continues to grow significantly. Inkjet printing has many advantages including low manufacturing costs, high quality output, enabling analogue-to-digital conversion, fast prototyping and compatibility with many different substrates (fragile, flexible or non-flat). Solvent-based inks are often preferred due to exceptional print quality, image durability and compatibility with a range of substrates. Such inks can be formulated with pigments or dyes. The main benefit of solvent-based inks is their good wetting ability to a variety of substrates with fast drying times,[2] but fast drying inks can be prone to block print head nozzles and the volatile organic

compounds (VOCs) utilized have detrimental effects on our health and the environment. In comparison, aqueous inks (often in combination with ethanol) are relatively inexpensive, environmentally friendly and are used extensively for desktop applications, where porous/specially treated substrates or lamination are used to improve the wettability of the substrate. However, aqueous inks often demonstrate poor adhesion to non-porous substrates used for many consumer products and suffer from slower drying times, limiting their suitability for industrial applications.

Polymeric materials have been exploited in aqueous inkjet formulations to successfully adhere aqueous-based inks onto hydrophobic substrates. These examples include the use of polymeric binders,[3–5] emulsion systems[6–8] and stimuli-responsive materials[6,9] to improve the gloss and durability of prints on plastics.[10] Our strategy to address this industrial problem is to design a single polymeric material that will allow aqueous-based inks to be printed onto hydrophobic substrates and become water-fast and durable after deposition. There are three main properties required for such a polymeric additive: (1) a hydrophilic component to enable aqueous-based ink formulations to be made, (2) hydrophobic character to provide affinity to hydrophobic substrates, and (3) a "triggerable" crosslinking moiety that can be activated after deposition by an external thermal stimulus to render the ink water-fast, offer improved anchoring to the substrate and deliver enhanced solvent, scratch and physical resistance.[11,12]

Reversible addition-fragmentation chain transfer (RAFT)[13–16] polymerization has been exploited to fabricate these block copolymers owing to its ability to synthesize a wide range of polymers with varying functionalities and architectures in a relatively straightforward way. Our group[17–20] and others[21–39] have demonstrated this versatility and have synthesized a plethora of functional polymers *via* RAFT polymerization. Of particular relevance, Hoogenboom *et al.*[40,41] have

previously reported the RAFT homopolymerization of 2-hydroxyethyl acrylate (HEA) in dimethylformamide (DMF) using dibenzyltrithiocarbonate (DBTTC) as a chain transfer agent (CTA). Well-defined PHEA homopolymers (mass dispersities, $Đ \leq 1.2$) with varying degrees of polymerization were successfully synthesized by tuning the feed molar ratio of HEA monomer to DBTTC and/or the reaction time. The same group also reported the RAFT (co)polymerization of HEA and 2-methoxyethyl acrylate (MEA), and a series of block and gradient copolymers with varying HEA/MEA content were synthesized with $Đ$ values in the range of 1.1 - 1.4.

Herein, we design polymers for use in industrial continuous inkjet (CIJ) printing. Our strategy exploits block copolymer solution self-assembly,[42–50] enabling the polymer to be processed from aqueous systems whilst still containing desired functionality to be printed onto hydrophobic substrates. Specifically, we utilize RAFT polymerization to synthesize a series of well-defined diblock copolymers with a hydrophilic block comprising statistically distributed 2-hydroxyethyl acrylate (HEA) and *N*-hydroxymethyl acrylamide (HMAA) residues and a hydrophobic poly(propyl methacrylate) (PPMA) block (see Scheme 1). Building on the work of Hoogenboom and co-workers, we explore two further trithiocarbonate CTAs (cyano-2-propyl dodecyl trithiocarbonate, CPDT, and 2-(dodecylthiocarbonothioylthio)-2-methylpropanoic acid, DCMP; see Scheme 1, inset) which are cheaper and less toxic than DBTTC. The HEA component imparts hydrophilic character to the polymer and HMAA is introduced as a second hydrophilic monomer that undergoes thermally-induced self-condensation reactions to generate covalent crosslinks.[31] Optimized polymerization conditions enabled the synthesis of well-defined P(HEA-*st*-HMAA) macro-CTAs, which were subsequently chain-extended with propyl methacrylate (PMA) to impart hydrophobic character and thus enhance interactions and adhesion with hydrophobic substrates.

The adhesive properties of the resulting amphiphilic P[(HEA$_x$-*st*-HMAA$_y$)-*b*-PMA$_z$] diblock copolymer additives were investigated for inkjet printing onto hydrophobic substrates.

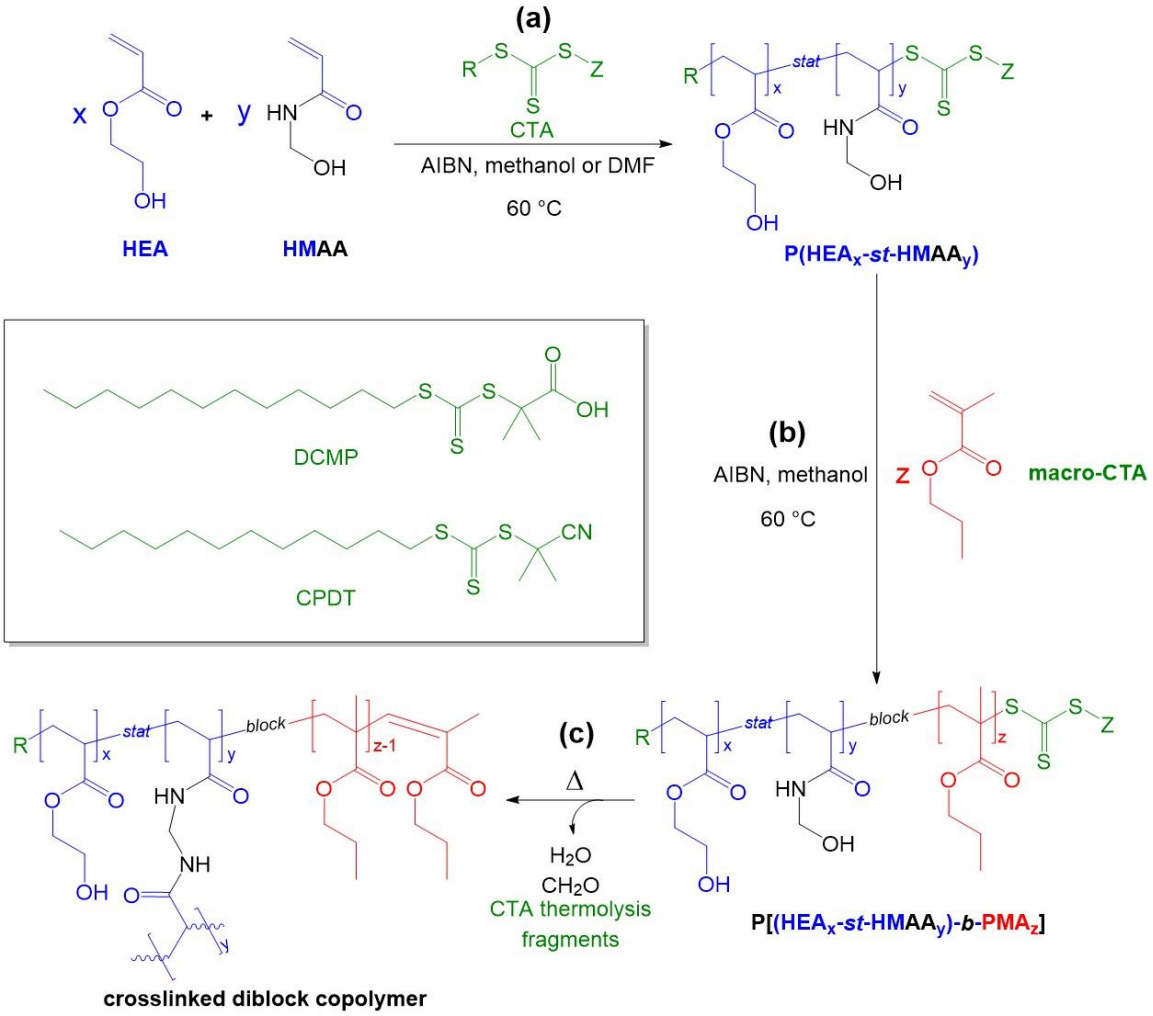

Scheme 1. (a) Synthesis of poly(2-hydroxyethyl acrylate-*stat*-*N*-hydroxymethyl acrylamide) by RAFT polymerization; (b) synthesis of poly[(2-hydroxyethyl acrylate-*stat*-*N*-hydroxymethyl acrylamide)-*b*-propyl methacrylate] using a poly(2-hydroxyethyl acrylate-*stat*-*N*-hydroxymethyl acrylamide) RAFT macro-CTA, (c) crosslinking via thermally-induced self-condensation of HMAA units within the hydrophilic block, where the major ether-bridged product is shown.[51] *N.B.* The CTA end fragment is likely to undergo thermolysis under the thermal conditions used during crosslinking forming an unsaturated chain end.[52]

Experimental

Materials

Dimethylformamide (DMF), methanol and *n*-hexane (all laboratory reagent grade) were purchased from Fisher Scientific and used as supplied. 2,2'-Azobis(isobutyronitrile) (AIBN), *t*-butanol, cyano-2-propyl dodecyl trithiocarbonate (CPDT) (≥ 97 %), deuterium oxide (D_2O), dimethylformamide (DMF, 99.8 %, anhydrous) and 2-(dodecylthiocarbonothioylthio)-2-methylpropanoic acid (DCMP, ≥ 97 %) were purchased from Sigma Aldrich and used without further purification. 2-Hydroxyethyl acrylate (HEA, ≥ 97 %), *N*-hydroxymethyl acrylamide (HMAA, 48% w/w in H_2O) and propyl methacrylate (PMA, ≥ 97 %) were purchased from Sigma Aldrich. Inhibitors were removed from HEA and PMA *via* a basic alumina column and water was removed from HMAA *via* freeze drying. d-Chloroform ($CDCl_3$, 99.8 % At + 0.05 % TMS), d_6-dimethyl sulfoxide (d_6-DMSO, 99.8 % At + 0.05 % TMS) were purchased from Goss Scientific and used as supplied. High-density polyethylene (HDPE), low-density polyethylene (LDPE), polypropylene (PP) and poly(ethylene terephthalate) (PET) substrates were purchased from Engineering & Design Plastics. Glycerol, 2-pyrrolidinone, Brilliant Blue dye, BYK-333, BYK-377, BYK-378, TEGO WET 500, Bon Jet CW-2, Cab-O-Jet, 1BK111, 2BK106-291BK, 2BK124-299BK and 433BL-104 were provided by Domino Printing Science PLC.

RAFT polymerization of 2-hydroxyethyl acrylate

The following example describes the polymerization of 2-hydroxyethyl acrylate (HEA) targeting a degree of polymerization (D_p) of 80 ($[AIBN]_0/[CTA]_0/[HEA]_0 = 0.2/1/80$) in methanol or DMF at 60 °C. A reaction tube suitable for a R. B. Radley Co. Ltd. Carousel 12 Plus, equipped with

a magnetic stirrer bar, was charged with a mixture of HEA (2 g, 17.2 mmol), CPDT (74 mg, 0.215 mmol), AIBN (7 mg, 0.04 mmol) and methanol/DMF (2 mL). The system was degassed three times *via* vacuum and nitrogen cycles, before the sealed tube under nitrogen atmosphere was placed into the 60 °C preheated carousel. Samples were taken at regular intervals and the monomer conversion measured via ^{1}H NMR spectroscopy and molar mass data by GPC. Termination of the reaction was achieved by exposing the reaction mixture to air and rapidly cooling by placing the reaction vessel into an ice bath. The polymer was precipitated by adding to stirring *n*-hexane (300 mL) dropwise. The *n*-hexane was then decanted and the resulting polymer was re-dissolved in methanol, transferred to a vial and the methanol was removed *via* rotary evaporation to yield a clear yellow viscous material.

RAFT polymerization of 2-hydroxyethyl acrylate and N-hydroxymethyl acrylamide

The following example describes the statistical copolymerization of 2-hydroxyethyl acrylate (HEA) and *N*-hydroxymethyl acrylamide (HMAA), targeting a total degree D_p of 80 ($[AIBN]_0/[CTA]_0/[HEA]_0/[HMAA]_0 = 0.2/1/76/4$) in methanol or DMF at 60 °C. A reaction tube suitable for a R. B. Radley Co. Ltd. Carousel 12 Plus, equipped with a magnetic stirrer bar, was charged with a mixture of HEA (2 g, 17.2 mmol), HMAA (91 mg, 0.90 mmol) CPDT (78 mg, 0.226 mmol), AIBN (7 mg, 0.04 mmol) and methanol (2 mL). The system was degassed three times *via* vacuum and nitrogen cycles, before the sealed tube under nitrogen atmosphere was placed into the 60 °C preheated carousel. Samples were taken at regular intervals and the monomer conversion measured *via* ^{1}H NMR spectroscopy and molar mass data by GPC. Termination of the reaction was achieved by exposing the reaction mixture to air and rapidly cooling by placing the reaction vessel into an ice bath. The polymer was

precipitated by adding the resulting polymer solution to *n*-hexane (300 mL) dropwise. The *n*-hexane was then decanted and the resulting polymer was re-dissolved in methanol, transferred to a vial and the methanol was removed *via* rotary evaporation to yield a clear yellow viscous material.

RAFT polymerization of propyl methacrylate

The following example describes the polymerization of propyl methacrylate (PMA) targeting a D_p of 20 ($[AIBN]_0/[CTA]_0/[PMA]_0 = 0.2/1/20$) in DMF at 60 °C. A reaction tube suitable for a R. B. Radley Co. Ltd. Carousel 12 Plus, equipped with a magnetic stirrer bar, was charged with a mixture of PMA (2 g, 16 mmol), CPDT (276 mg, 0.80 mmol), AIBN (24 mg, 0.15 mmol) and DMF (2 mL). The system was degassed three times *via* vacuum and nitrogen cycles, before the sealed tube under nitrogen atmosphere was placed into the 60 °C preheated carousel. Samples were taken at regular intervals and the monomer conversion measured *via* ^{1}H NMR spectroscopy and molar mass data by GPC. Termination of the reaction was achieved by exposing the reaction mixture to air and rapidly cooling by placing the reaction vessel into an ice bath. The polymer was precipitated by adding the resulting polymer solution to methanol (300 mL) dropwise; the precipitate was filtered and washed with methanol resulting in a yellow powder.

Synthesis of poly[(2-hydroxyethyl acrylate*-st-N-*hydroxymethyl acrylamide)*-b-*propyl methacrylate] via RAFT polymerization, P(HEA*-st-*HMAA)*-b-*PPMA

The following example describes the polymerization of propyl methacrylate using a poly(HEA_x-*st*-$HMAA_y$) macro-CTA targeting a PPMA D_p of 20 ($[AIBN]_0/[\text{macro-CTA}]_0/[PMA]_0 = 0.2/1/20$)

in methanol at 60 °C. A round bottom flask, was charged with a mixture of PMA (128 mg, 1.00 mmol), macro-CTA (1 g, 0.05 mmol), AIBN (1.6 mg, 0.01 mmol) and methanol (2 mL). The system was degassed three times *via* vacuum and nitrogen cycles, before the sealed tube under nitrogen atmosphere was placed into the 60 °C preheated oil bath. Samples were taken at regular intervals and the monomer conversion measured *via* ^{1}H NMR spectroscopy and molar mass data by GPC. Termination of the reaction was achieved by exposing the reaction mixture to air and rapidly cooling by placing the reaction vessel into an ice bath. The polymer was precipitated by adding the resulting polymer solution to *n*-hexane (300 mL) dropwise. The *n*-hexane was then decanted and the resulting polymer was re-dissolved in methanol, transferred to a vial and the methanol was removed *via* rotary evaporation to yield a clear yellow viscous material.

Crosslinking studies

Crosslinking tests were performed in both the bulk and thin film to ascertain the time required for the polymers to form an insoluble network. Polymer samples in the bulk were placed in an oven at 150 °C and samples removed at set time intervals to be tested for their solubility in methanol. A modified thin film method was implemented in order to mimic conditions of the printing process. Drop cast films of the copolymer (from ethanol/water 50:50 w/w) on PTFE substrates were prepared and the crosslinking conditions investigated as with bulk samples. All samples were left to dry for 3 hours at room temperature before heating.

Characterization

^{1}H NMR spectroscopy was performed using a 300 MHz Bruker Avance Spectrometer. Samples were dissolved in d_6-DMSO or $CDCl_3$. ^{1}H NMR was used to calculate monomer conversion throughout the polymerizations. *Gel permeation chromatography (GPC)* was performed on an Agilent GPC 50 plus consisting of two PL gel 5 µm 300 x 7.5 mixed-C columns as well as a guard column. The mobile phase used was degassed DMF containing 0.10% w/v LiBr, at a flow rate of 0.8 mL min^{-1} and the column oven set to 50 °C. Calibrations were performed using near monodispersed poly(methyl methacrylate) (M_p range = 690 to 1,944,000 gmol^{-1}). Samples were prepared by dissolution in DMF eluent (approximately 4 mg mL^{-1}) and filtered using a 0.45 µm Millipore syringe filter. Toluene was used as a flow rate marker. Cirrus GPC software (version 3.2) provided by Agilent technologies was used to analyze the data. *Fourier transform infrared (FTIR)* spectra of all the samples were obtained using attenuated total reflectance (ATR) on a Thermo Nicolet 380 FTIR spectrophotometer over the range 4000-500 cm^{-1} for 16 scans with a resolution of 4 cm^{-1}. *Dynamic light scattering (DLS)* measurements were performed using a Malvern Zetasizer Nano ZS instrument. Z-average and polydispersity were measured using approximately 1 mL of solution in a polystyrene cuvette. Each sample was analyzed 3 times with 12 scans in each run. The instrument is verified monthly using an aqueous polystyrene latex (Z-average 290 ± 10 nm) verification standard. Surface tension of polymer solutions were measured using a SITA pro line t15 bubble tensiometer where the surface tension was measured over a pre-selected range of bubble lifetimes. The instrument was calibrated with deionized water before each measurement. Viscometry measurements of polymer solutions were performed using a Brookfield ball drop tensiometer. Measurements were recorded 5 times over a range of angles (20°, 30°, 40°, 50°, 60°, 70° and 80°).

Adhesion tests

Adhesive performance was tested on polymer and ink formulations on substrates after drying, with and without crosslinking. A range of industrially-designed tests were first employed to qualitatively measure the adhesive properties of the block copolymers and ink formulations on various substrates [poly(ethylene terephthalate) (PET), polypropylene (PP), high-density polyethylene (HDPE), low-density polyethylene (LDPE) and glass]. These tests, although not fully quantitative, allow the printing industry to screen the adhesion between inks and substrates that are intended for use as prints on commercial food packaging. 5% w/w polymer solutions in methanol:water (50:50 w/w) were drawn down onto the substrates using a 6 μm K-bar and dried for 3 hours at ambient temperature in the fume cupboard. Wetting of the polymer onto the substrate was assessed visually using a 10 x 10 grid drawn on a transparent film, which was placed on top of the draw down to calculate the approximate percentage coverage of the substrate before and after crosslinking. The adhesive performance was qualitatively measured by the number of rubs (using a blunt, rounded surface, typically a thumb) and scratches (using a sharper, more penetrating tool, like a spatula) needed to remove the ink from the substrate. Approximately equal force was used each time and tests were done in triplicate. 'Tape tests' were performed whereby a 10 x 10 grid of squares (25 cm^2 total area) was cut into the ink/polymer. A suitable length of 3M Scotch Tape (both 610 and 810, where by 810 has a stronger adhesive force than 610) was used to cover the area surrounding the pattern as well as leaving an untethered free area of tape (approximately 5 cm^2) for subsequent removal. The tape was applied carefully to avoid creases and air bubbles. One hand was used to hold

the unattached tail portion of tape and the tape was removed with a swift motion that combines both lifting and pulling action, attempting to maintain consistency between samples. Again, tests were repeated two additional times to obtain suitable average values for each polymer system.

Each of these tests was assessed by a qualitative rating system (0 to 10, where 10 shows the highest adhesive performance), where the five scores are best illustrated by radar plots to observe overall performance (see ESI for details). Rub and scratch tests were assessed by the number of rubs (or scratches) before the ink was removed from the substrate. Greater than 10 rubs was considered excellent and has the highest score of 10, 8 - 10 rubs was considered good and has a score of 8, 5 – 8 rubs moderate and has a score of 6, 3 - 5 poor and has a score of 4 and less than 3 rubs is considered very poor and has a score of 2. For the tape tests this was assessed by the percentage of ink removed (measured from the number of squares of the grid removed) from the substrate. Where 0 – 20 % removal was considered excellent and has a score of 10, 20 - 40 % good and has a score of 8, 40 - 60% rubs moderate and has a score of 6, 60 – 80% poor and has a score of 4, and more than 80 % is considered very poor and has a score of 2. 100 % removal would have a score of zero.

Quantitative lap-shear adhesive performance was assessed on the four block copolymers that performed the best in the qualitative industry adhesion tests {namely P[(HEA$_{72}$-*st*-HMAA$_8$)-*b*-PMA$_{20}$], P[(HEA$_{72}$-*st*-HMAA$_8$)-*b*-PMA$_{40}$], P[(HEA$_{108}$-*st*-HMAA$_{12}$)-*b*-PMA$_{20}$] and P[(HEA$_{108}$-*st*-HMAA$_{12}$)-*b*-PMA$_{40}$]}, before and after crosslinking, using a linear test machine (3300 model, TA Instruments, New Castle, DE, USA). Polymer (50 mg) was placed in between overlapping PP substrates (700 mm x 150 mm x 1.5 mm) where the polymer

covered overlap was 150 mm^2. A 500 g weight was placed on the upper substrate, directly above the polymer interlayer, for 3 hours. To crosslink the polymers, the samples were placed in an oven at 150 °C for 3 hours. Samples were placed in the test machine grips and the substrates pulled apart at a constant rate of 10 mm min^{-1}, until the substrates were separated from one another.

Ink Formulations

In order to test the performance of the block copolymers in continuous ink jet (CIJ) printing the polymers were incorporated into ink formulations. 5% w/w polymer and 1% w/w brilliant blue dye were dissolved in ethanol:water 50:50 w/w and shaken for approximately 1 hour. Ink formulations were filtered through a 0.2 µm filter before jetting.

Results and Discussion

Extensive scouting experiments were conducted in order to develop a scalable polymerization formulation that enables control over the total molecular weight of the hydrophilic P(HEA-*st*-HMAA) block, the triggerable crosslinking performance (by controlling the HMAA monomer loading within the hydrophilic block) and the overall hydrophobic/hydrophilic balance of the block copolymer (to control the aqueous dispersibility). Controlling these parameters allows for tailoring of the final properties of the polymers and thus provide optimum performance in aqueous inkjet printing. Accordingly, two appropriate trithiocarbonate chain transfer agents (CTAs) were investigated (cyano-2-propyl dodecyl trithiocarbonate, CPDT, and 2-(dodecylthiocarbonothioylthio)-2-methylpropanoic acid, DCMP) in two polar solvents

(methanol and DMF). These CTAs were selected as they have been shown to be effective in the controlled polymerization of more-activated monomers (MAMs).[53,54]

Synthesis of poly(2-hydroxyethyl acrylate), PHEA

Firstly, control over the RAFT homopolymerization of HEA was studied to identify optimum synthesis conditions (see Table S1 and Figures S1 to S3 for the molecular mass data, kinetic plots and GPC traces of each of the four systems). Using both CPDT and DCMP enabled high monomer conversions to be achieved in both solvents, whilst providing good control over the final molecular mass with low mass dispersities ($Đ < 1.16$) observed. GPC analyses indicated that formulations yielded polymers of similar molecular mass that was approximately twice as large as the theoretical target. This was attributed to the differing polarities and radii of gyration in DMF of PHEA as compared to the PMMA standards used in the GPC calibration.[55] The GPC traces also exhibited a small high molecular weight shoulder. This could be a consequence of one, or a combination of, the following: (i) dipole interactions between the polymer and DMF, as observed elsewhere[55] (LiBr has been incorporated to minimize this effect as much as possible); (ii) light branching as a consequence of diacrylate impurity in the monomer batch; and/or (iii) the copolymerization of macromonomer formed by the propagating radical undergoing backbiting β-scission, which occurs significantly during the radical polymerization of acrylates (particularly when pushed to high monomer conversion).[56] Given that methanol and DMF can be successfully employed in the controlled polymerization of PHEA, methanol was selected for all subsequent polymerizations to negate the extensive drying times required for DMF and the association of DMF with developmental toxicity and carcinogenic effects.[57]

Important initial investigations of P[(HEA-*st*-HMAA)-*b*-PMA] syntheses highlighted that CPDT outperformed DCMP as an efficient CTA. When using CPDT, block copolymers with molar mass dispersities ≤ 1.23 were achieved, demonstrating good RAFT control. Conversely, when using DCMP, the resulting block copolymers exhibited near-identical M_n values to those synthesized with CPDT, but showed significantly less control over the molecular weight distribution ($Đ \leq 1.38$, see Table S2 and Figure S4).

Synthesis of poly(2-hydroxyethyl acrylate-stat-N-hydroxymethyl acrylamide), P(HEA-st-HMAA)

The HMAA loading within P(HEA-*st*-HMAA) hydrophilic copolymers (total degree of polymerization, $D_p = 80$) was systematically varied in order to control their crosslinking behavior. Table 1 shows the results obtained for the copolymerization of HEA and HMAA at varying molar ratios in methanol using CPDT. Relatively high monomer conversions (≥ 88 %, with all but one greater than 90% after 4 hours polymerization time) were achieved, and the resulting copolymers exhibited low mass dispersities ($Đ \leq 1.18$ in all cases), with the $Đ$ values increasing slightly on increased HMAA loading.

Table 1. Molar mass data for the RAFT copolymerization of HEA and HMAA using CPDT in methanol.

Target PHEA D_p	Target PHMAA D_p	Total monomer conversion[a] (%)	$M_n^{th,b}$ (g mol^{-1})	M_n^c (g mol^{-1})	$Đ$ [M_w/M_n][c]
80	0	98	9,449	22,400	1.11
79	1	98	9,434	21,800	1.12
77	3	96	9,220	19,600	1.13
76	4	88	8,467	19,200	1.16
72	8	97	9,239	17,800	1.18
70	10	93	8,845	21,300	1.18

a) Determined by ^{1}H NMR spectroscopy

b) Theoretical molecular weight of polymer calculated using Equation S2– see ESI

c) Determined by DMF GPC using poly(methyl methacrylate) standards (see Figure S5 for traces)

FTIR spectroscopy was utilized as a simple analytical tool to approximate the extent of HMAA loading in the hydrophilic polymer following precipitation (see Figure 1). The intensity of the N-H bending band in HMAA (1600-1500 cm^{-1}) was compared with the sp^3 C-H bands (3000-2850 cm^{-1}) arising from both repeat units in the polymer and correlated with the target HMAA loading. Figure 1(c) shows that there is an approximately linear relationship between the ratio of the bands and the amount of HMAA. This correlation allows the HMAA content for any of our copolymers with a D_p 80 to be approximately calculated. It should be noted that this is merely a qualitative guide to verify the successful incorporation of the expected quantity of HMAA.

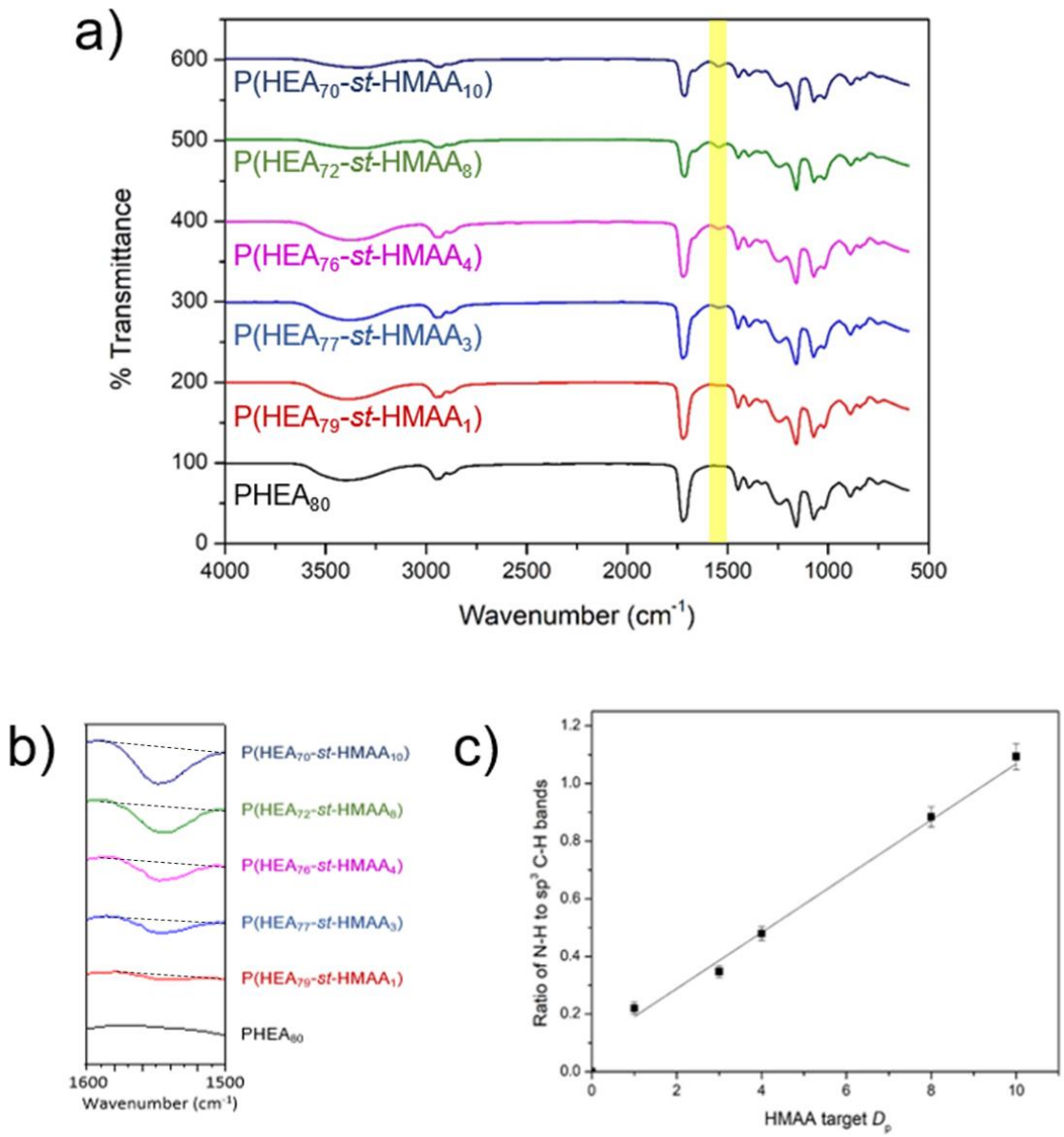

Figure 1. (a) FTIR spectra for copolymers containing HMAA, where the absorbance corresponding to N-H bending at 1600 – 1500 cm^{-1} has been highlighted in yellow and expanded in (b). (c) Difference in absorbance between N-H and sp^3 hybridized C-H bands for copolymers containing different amounts of HMAA (error bars represent the range of three repeats).

In order to study the effects of HMAA loading on crosslinking performance, experiments were performed in both bulk and thin film whereby the solubility of the polymers was tested in methanol

after heating to 150 °C for varying amounts of time (see Tables S3 to S5). Bulk testing involved placing a sample of the purified dry polymer in an oven at 150 °C whereas thin film crosslinking was designed to be closer to the conditions of the printing process. Drop cast films of the copolymer (from ethanol/water 50:50 w/w) on polytetrafluoroethylene (PTFE) substrates were prepared and subsequently heated in an oven at 150 °C to compare their crosslinking ability. Samples were allowed to dry for 3 hours at room temperature before heating.

As expected, increasing the HMAA loading decreased the required crosslinking time, with only 10 mol% needed to reduce the crosslinking time to below 10 minutes (for a copolymer with a total degree of polymerization of 80) in the bulk. Thin film samples took significantly longer to crosslink, where P(HEA_{72}-*st*-$HMAA_{10}$) (14 mol% HMAA) required just over one hour at 150 °C. It is noteworthy that higher HMAA loadings were difficult to obtain due to *in situ* crosslinking during polymerization.

To further investigate the control of molecular mass of the hydrophilic crosslinkable block, a range of P(HEA-*st*-HMAA) polymers with varying D_p were synthesized at fixed HMAA loading (10 mol%), using CPDT and DCMP (Table S6 and Figure S6). Both CTAs allow the synthesis of copolymers with a range of M_n values (target D_p of 40, 80 and 120) and low molar mass dispersities ($Đ < 1.2$), with all polymerizations proceeding to high monomer conversion (≥ 96%). One could argue that CPDT performed marginally better than DCMP in these polymerizations, but the enhanced performance (lower molar mass dispersities and higher monomer conversion) is minimal and lies within expected experimental error. Due to the significant peak overlap of HEA, HMAA and the CTA, ^{1}H NMR spectroscopy could not be used to determine the HMAA loading in the block copolymers. FTIR spectroscopy indicated that the HMAA loading was ± 2% of the target of

10 mol% in each case (see Figure S7) and this value increases slightly with increased molecular mass, while CPDT exhibits marginally better control over HMAA loading than DCMP.

The two CTAs used during the synthesis of the hydrophilic block were then screened for the synthesis of the hydrophobic poly(propyl methacrylate), PPMA, block (target D_p of 20) in DMF. Higher monomer conversion was achieved when using CPDT (93%) compared to DCMP (76%), and CPDT also facilitated the synthesis of $PPMA_{20}$ with significantly lower molar mass dispersity ($Đ$ = 1.12 *vs.* 1.27), as shown in Table S7 and Figures S8 and S9. Finally, a series of systematic experiments revealed that the optimum route to synthesize these triggerable block copolymers was *via* the synthesis of a CPDT-based P(HEA-*st*-HMAA) macro-CTA, followed by the polymerization of PMA, employing methanol as the solvent in both steps (see Table S2 and Figure S4). The determined optimal order in which each monomer should be polymerized was expected when considering the relative monomer propagation rates, which has been extensively discussed by Keddie elsewhere.[57] It should also be noted that methanol could not be used as a solvent when using a PPMA macro-CTA due to poor solubility.

Synthesis of crosslinkable poly[(2-hydroxyethyl acrylate-stat-N-hydroxymethyl acrylamide)-block-propyl methacrylate], P(HEA-st-HMAA)-b-PPMA, amphiphilic block copolymers

Once the optimum route for the synthesis of P[(HEA-*st*-HMAA)-*b*-PMA] was identified, three families of block copolymers were synthesized. The HMAA loading was fixed at 10 mol% of the hydrophilic block whilst the molar mass ratio of the hydrophilic to hydrophobic block was varied (both hydrophilic and hydrophobic block lengths were systematically varied, as shown in Table 2). Importantly, the hydrophilic macro-CTAs were synthesized on a relatively large scale (20 g) to facilitate the synthesis of sufficient quantities of block copolymer for use in industrial trials. The

monomer conversions were 97 – 98% for all three macro-CTAs and the molar mass dispersities were only slightly higher than those obtained for the equivalent small-scale syntheses ($Đ$ = 1.20 – 1.21 *vs.* 1.17 – 1.18, see Table S8 and S6, respectively). Importantly, the HMAA loadings achieved were within 1 mol% of those targeted. Additionally, GPC analyses of the P[(HEA$_x$-*st*-HMAA$_y$)-*b*-PMA$_z$] block copolymers indicated minimal contamination of 'dead' macro-CTA chains (those without RAFT chain-end functionality) in the final product (see Figure 2), clearly demonstrating that successful unimodal chain extension with PMA was achieved. The relative PPMA D_p values (as calculated using DMF GPC against PMMA standards, Table 2) were close to the target D_p. Notably, longer polymerization times were required to obtain suitably high monomer conversion (>85 % in all cases) when targeting longer PPMA blocks.

Table 2. Molar mass data for the RAFT polymerization of PMA using a CPDT-based P(HEA_x-*st*-$HMAA_y$) macro-CTA in methanol

macro-CTA				Target PPMA D_p	Target M_n (g mol^{-1})	Time (h)	Actual PPMA D_p	M_n [a] (g mol^{-1})	Monomer Conv. (%)[c]	$Đ$ [M_w/M_n][a]
Block composition	**M_n [a] (g mol^{-1})**	**$Đ$ [a] [M_w/M_n]**	**HMAA mol%[b]**							
P(HEA_{36}-*st*-$HMAA_4$)	9,900	1.20	9.8	5	10,500	96	6	10,700	95	1.21
				10	11,200	120	12	11,400	92	1.24
				20	12,500	120	*	*	*	*
				40	15,000	120	*	*	*	*
P(HEA_{72}-*st*-$HMAA_8$)	17,200	1.21	10.2	5	17,800	96	4	17,700	91	1.21
				10	18,500	120	12	18,700	93	1.23
				20	19,800	120	19	19,600	90	1.23
				40	22,300	144	35	21,700	85	1.25
P(HEA_{108}-*st*-$HMAA_{12}$)	24,000	1.21	10.7	5	24,600	96	5	24,600	94	1.21
				10	25,300	120	13	25,700	90	1.23
				20	26,600	120	21	26,700	92	1.24
				40	29,100	144	36	28,600	87	1.25

a) Determined by DMF GPC using poly(methyl methacrylate) standards

b) Estimated by FTIR spectroscopy

c) Estimated (due to large overlap with HEA and HMAA peaks) by ^{1}H NMR spectroscopy

* Polymers precipitated out during synthesis due to poor solubility with larger hydrophobic blocks

Polymers with the shortest hydrophilic block in combination with longer targeted hydrophobic blocks, namely P(HEA_{36}-*st*-$HMAA_4$)-*b*-PMA_{20} and P(HEA_{36}-*st*-$HMAA_4$)-*b*-PMA_{40}, could not be synthesized using the developed method because the polymers precipitated during the growth of PPMA due to their poor solubility in methanol. If desired, these polymers could be synthesized under emulsion or dispersion conditions (as demonstrated elsewhere for other amphiphilic block copolymers[49,58,59]), but given that the P(HEA_{36}-*st*-$HMAA_4$) family performed the worst in the adhesion tests (*vide infra*), this was not pursued.

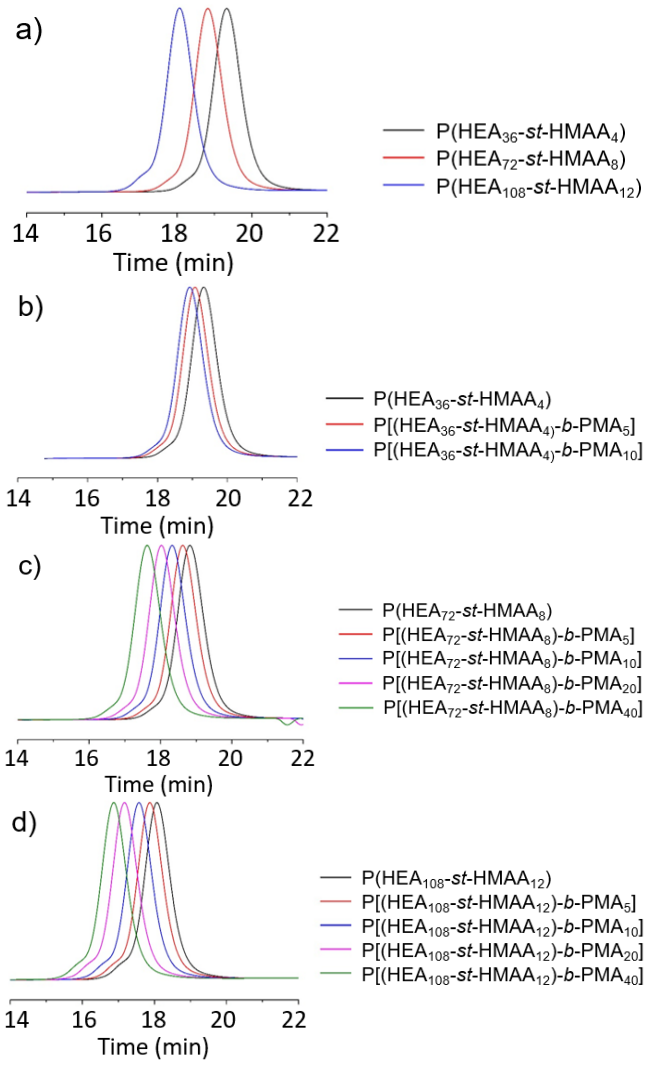

Figure 2. GPC traces of (a) P(HEA$_x$-*st*-HMAA$_y$) macro-CTAs, and P[(HEA$_x$-*st*-HMAA$_y$)-*b*-PMA$_z$] block copolymers synthesized using (b) P(HEA$_{36}$-*st*-HMAA$_4$), (c) P(HEA$_{72}$-*st*-HMAA$_8$) and (d) P(HEA$_{108}$-*st*-HMAA$_{12}$) macro-CTAs.

A crosslinking study was performed in both the bulk and thin film (drop-cast) for all block copolymers in order to investigate the effect of molecular weight on required crosslinking times. More specifically, the HMAA hydrophilic monomer units can undergo thermally-induced self-condensation reactions to generate covalent crosslinks between HMAA units within the system[31] (see Scheme 1c). Samples were placed in an oven at 150 °C for varying times before being

evaluated for their solubility in methanol to determine when successful crosslinking had occurred (see Figure 3 and Table S9). These block copolymers exhibited the same trend as the hydrophilic macro-CTA statistical copolymers (see Tables S3 and S4), with longer crosslinking times being required in the thin film geometry compared to the bulk, which could be attributed to decreased mobility in the thin films (this phenomenon is the subject to ongoing studies in the group). The required crosslinking time was reduced with increased polymer molecular weight (even when the D_p of the hydrophobic, non-crosslinking, PPMA block is increased and thus the total HMAA content is reduced), which may be attributed to longer polymer chains having increased entanglement and less local mobility, which increases the probability of HMAA-HMAA interactions (*vide infra*).

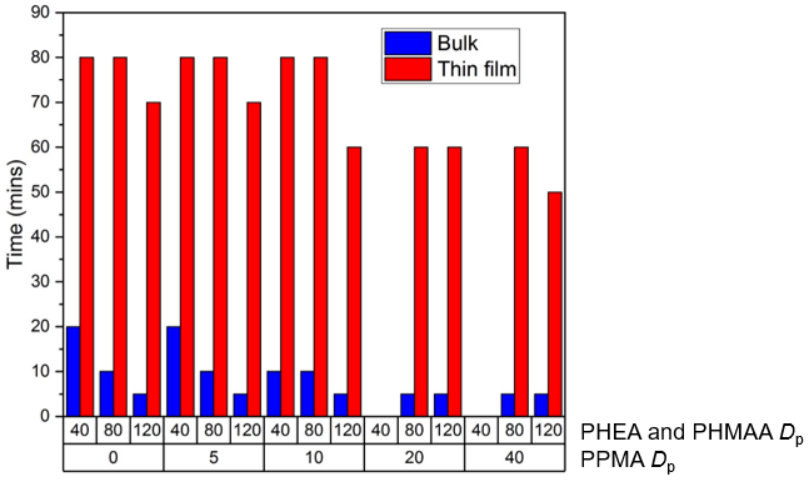

Figure 3. Maximum required crosslinking times for P(HEA_x-*st*-$HMAA_y$) macro-CTAs and P[(HEA_x-*st*-$HMAA_y$)-*b*-PMA_z] block copolymers in bulk (blue bars) and drop-cast films (red bars). In all cases, the HMAA loading was ~10 mol% with respect to the HEA content.

Industrial adhesive analysis

Qualitative adhesive tests were performed on all P[(HEA_x-*st*-$HMAA_y$)-*b*-PMA_z] block copolymers in the series. Polymer films were cast onto poly(ethylene terephthalate) (PET, Figure 4) and polypropylene (PP, Figure 5) before and after crosslinking (150 °C, 3 hours) to screen the polymers and examine the effects of molecular weight, hydrophobic block length and crosslinking. Five industrial adhesive tests were employed, as described in the Experimental section, to fully examine the range of abrasive interactions that printed food packaging products undergo during their useable life-cycle. Films were subjected to (A) wetting (water:methanol 50:50 w/w); (B) finger rub; (C) nail scratch; (D) tape 610 peel-off and (E) tape 810 peel-off (where 810 has higher adhesive strength than that of 610). Figures 4 and 5 show that the block copolymers adhered better to PET than PP, both before and after crosslinking. As expected, this shows that our (meth)acrylic amphiphilic block copolymers are more suited to the more polar, ester-containing PET substrate than the apolar polyolefin, PP, surface. More crucially, this series of screening tests shows that crosslinking significantly improves the adhesive properties. The thermal treatment used here induces two distinct processes: (i) generation of a covalently crosslinked polymer network (*via* self-condensation of the HMAA units in the hydrophilic block) with enhanced resistance to solvent and physical damage, and (ii) migration of the hydrophobic PPMA blocks (*via* thermal annealing) to increase their interactions with the hydrophobic substrate (both PET and PP).[60,61] Accordingly, there was improved adhesion on both substrates as the PPMA block length is increased, supporting

the notion that the pendent alkyl chains from the propyl methacrylate groups enhance the hydrophobic–hydrophobic interactions between the polymer and the substrate.

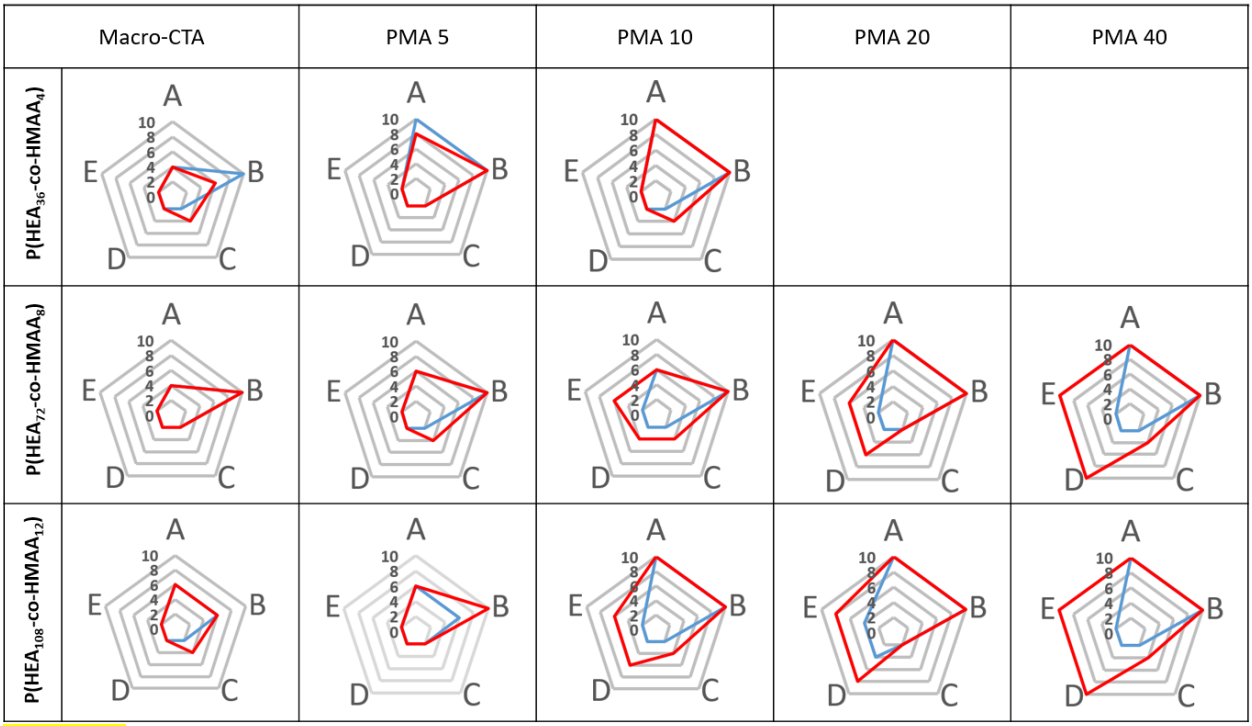

Figure 4. Adhesive properties of various P[(HEA$_x$-*st*-HMAA$_y$)-*b*-PMA$_z$] block copolymer drawn down films on PET before (blue) and after (red) crosslinking *via* heating at 150 °C for 3 h. A – wetting, B – finger rub, C – nail scratch, D – tape 610 and E – tape 810. *N.B.* The crosslinked polymer area (red) is bigger than the non-crosslinked area (blue) in all cases except for P(HEA$_{36}$-*st*-HMAA$_4$) and P[(HEA$_{36}$-*st*-HMAA$_4$)-*b*-PMA$_5$], where the non-crosslinked polymer outperforms the crosslinked polymer in one or two of the tests, and P(HEA$_{72}$-*st*-HMAA$_8$), where both polymers perform equally in all tests.

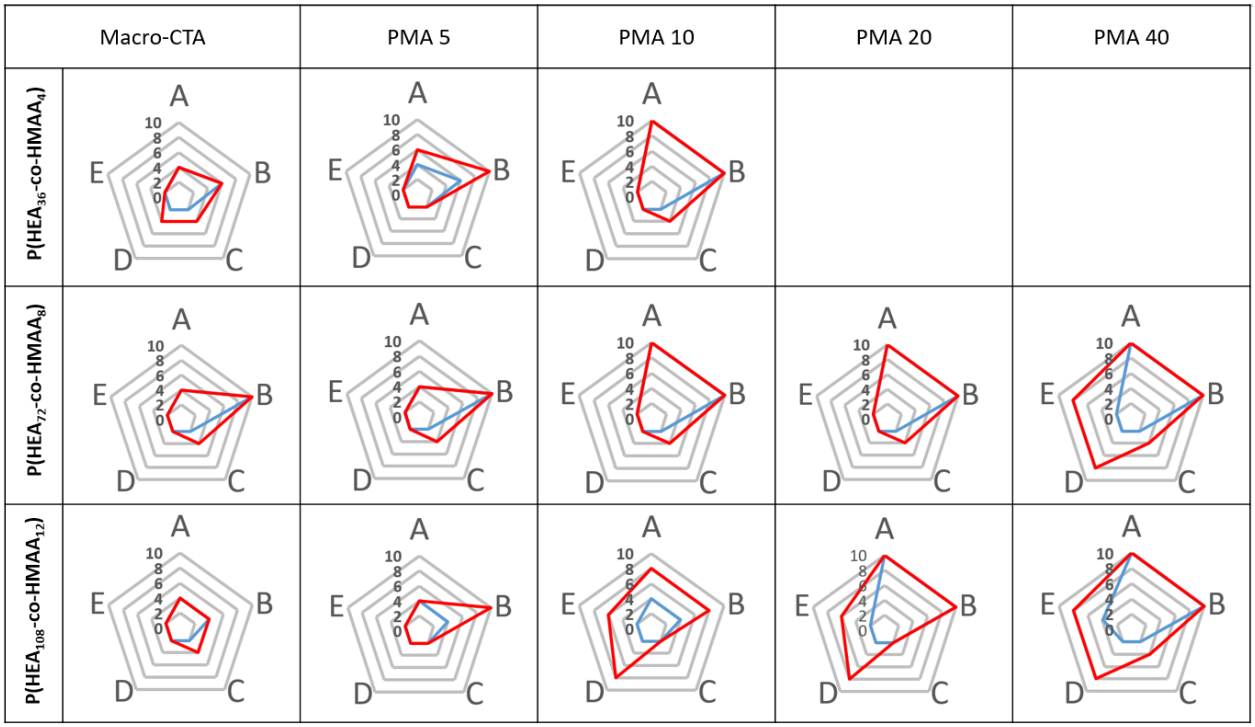

Figure 5. Adhesive properties of P[(HEA$_x$-*st*-HMAA$_y$)-*b*-PMA$_z$] block copolymer drawn down films on PP before (blue) and after (red) crosslinking *via* heating at 150 °C for 3 h. A – wetting, B – finger rub, C – nail scratch, D – tape 610 and E – tape 810.

These screening tests demonstrate that greater hydrophobic block volume fractions provide enhanced adhesive properties. In summary, with the desire to reduce crosslinking times as much as possible (< 60 minutes in thin film), the most important molecular design parameters for promising block copolymer ink additives are: (i) a high HMAA content (12.5 mol% HMAA within the hydrophilic block was shown to provide the maximum possible loading without promoting crosslinking events during polymerization), (ii) a long hydrophilic block (which reduces the required crosslinking time to below 60 minutes), and (iii) a high hydrophobic block volume fraction. Accordingly, quantitative lap-shear adhesive tests (with PP substrates) were performed on the four block copolymers that fit these design parameters, namely P[(HEA$_{72}$-*st*-HMAA$_8$)-*b*-

PMA$_{20}$], P[(HEA$_{72}$-*st*-HMAA$_{8}$)-*b*-PMA$_{40}$], P[(HEA$_{108}$-*st*-HMAA$_{12}$)-*b*-PMA$_{20}$] and P[(HEA$_{108}$-*st*-HMAA$_{12}$)-*b*-PMA$_{40}$], as shown in Figure 6.

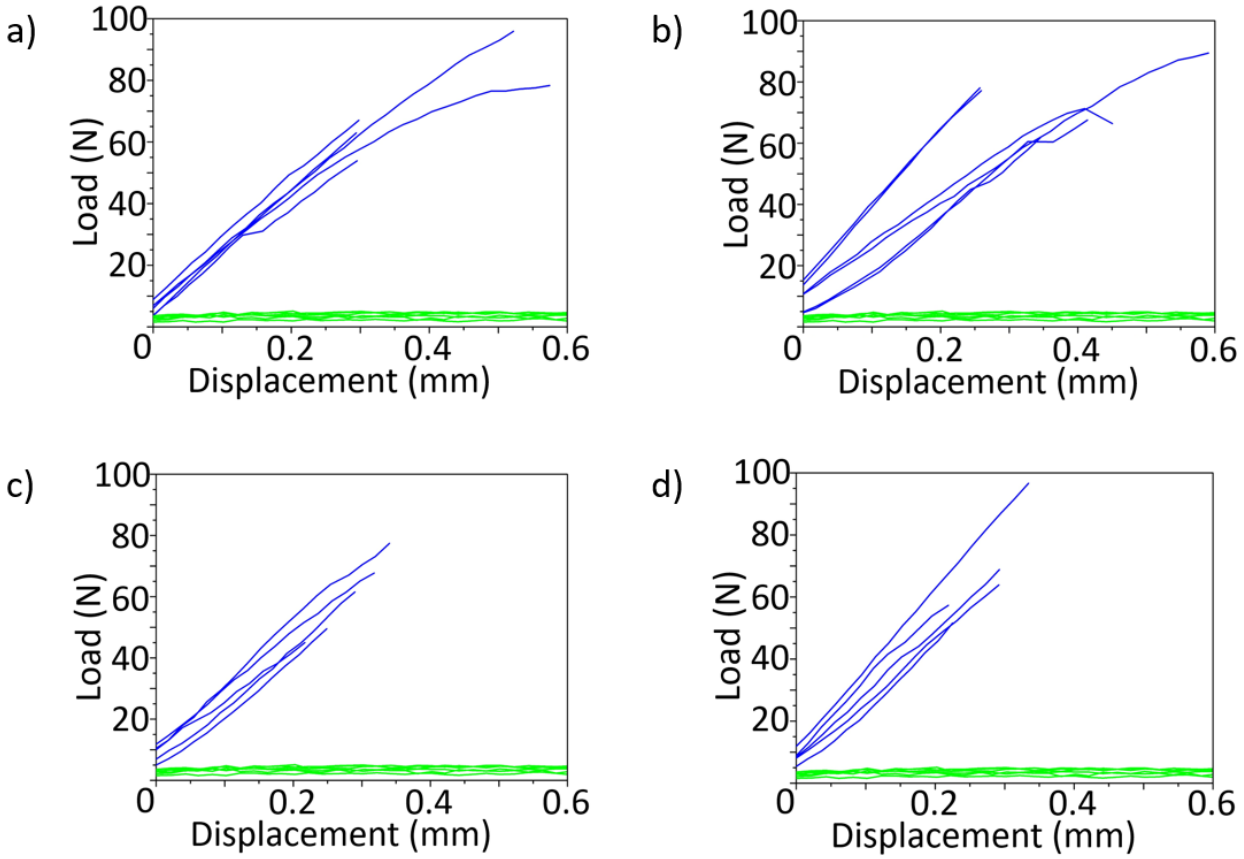

Figure 6. Load *vs.* displacement for crosslinked (blue) and non-crosslinked (green) P[(HEA$_x$-*st*-HMAA$_y$)-*b*-PMA$_z$] block polymers. (a) P[(HEA$_{72}$-*st*-HMAA$_{8}$)-*b*-PMA$_{20}$], (b) P[(HEA$_{72}$-*st*-HMAA$_{8}$)-*b*-PMA$_{40}$], (c) P[(HEA$_{108}$-*st*-HMAA$_{12}$)-*b*-PMA$_{20}$] and (d) P[(HEA$_{108}$-*st*-HMAA$_{12}$)-*b*-PMA$_{40}$].

All four polymers performed similarly in the lap-shear tests (see Figure 6). The most striking observation was the difference between crosslinked and non-crosslinked polymers. The mean average load at failure (for all four polymers) during the lap-shear tests for crosslinked and non-

crosslinked polymers was 67.2 ± 14.1 N and 4.1 ± 1.3 N, respectively. Crosslinked and non-crosslinked polymers also exhibited different modes of failure. Non-crosslinked samples exhibited cohesive failure, i.e. the polymer itself failed (polymer residue remained on both parts of the substrate). Conversely, the crosslinked polymer samples underwent adhesive failure, *i.e.* the failure occurred at the polymer-substrate interface (all the polymer remained on one part of the substrate and the other was devoid of polymer) (see Figure S10). The crosslinking process strengthens the polymer itself, but also binds the polymer more strongly to the hydrophobic substrate. Crosslinked polymers with higher PMA content appeared to require a larger force to cause adhesive failure; P[(HEA$_{72}$-*st*-HMAA$_{8}$)-*b*-PMA$_{40}$ failed at a mean average of 73.3 ± 10.6 N compared to 71.6 ± 16.2 N for P[(HEA$_{72}$-*st*-HMAA$_{8}$)-*b*-PMA$_{20}$], and P[(HEA$_{108}$-*st*-HMAA$_{12}$)-*b*-PMA$_{40}$] failed at a mean average load of 67.5 ± 17.5 N compared to 56.4 ± 13.2 N for P[(HEA$_{108}$-*st*-HMAA$_{12}$)-*b*-PMA$_{20}$], but these differences are all within one standard deviation.

Ink formulation and printability

Viscosity measurements were obtained to test the printability of the four block copolymers at 5% w/w (see Table S10), where the viscosity range for printing has been found to be 3 - 10 mPa.s.[62] Addition of the polymers (5% w/w) to ethanol:water mixtures (50/50 w/w) resulted in a viscosity increase from 2.4 mPa.s, but importantly remained within the printable viscosity range (3.7 mPa.s $\leq \eta \leq$ 5.6 mPa.s)[10] and could therefore be incorporated into inkjet formulations. Dynamic light scattering (DLS, Figure S11 and Table S11) performed on these solutions indicated that the four block copolymers assemble into micellar aggregates with a unimodal, albeit relatively polydisperse, distribution of hydrodynamic diameters ranging from 330 to 480 nm (PDI values 0.23-0.33). The block copolymers with longer hydrophilic blocks aggregated to form larger

particles, which was attributed to the hydrophobic nature of the CPDT CTA Z-group affecting the aggregation of the block copolymers in solution since this end-group will strive to avoid unfavorable interactions with the solvent. As the Z-group is relatively small compared to the hydrophilic polymer block, a great number of Z-groups can aggregate and form the core of the micelle, resulting in an increased number of polymer chains and therefore a large micellar structure. However, as the hydrophobic PPMA D_p increases, the effect of the CTA Z-group on self-assembly is reduced, resulting in smaller uniform micelles. Similar observations have also been reported by Armes and co-workers.[63]

Ink formulations based on industrial standards at Domino Printing Sciences were prepared using the four block copolymers and the dye '*Brilliant Blue*' (see Figure S12 for the chemical structure). For our continuous inkjet (CIJ) printing study, we have deliberately chosen to study simple formulations (solely comprising: solvent, dye and block copolymer at 5% w/w). Additionally, a standard Domino Printing Sciences ink formulation containing solvent and dye alone was also used for comparison and is referred to herein as 433BL. Details of the formulation compositions, their solution properties and jetting performance are described in detail in the Supporting Information (Tables S12-15 and Figures S13 and S14). In short, P[(HEA$_{108}$-*st*-HMAA$_{12}$)-*b*-PMA$_{20}$] (contained in formulation CF1) exhibited similar droplet shapes during printing to the commercial ink formulation (without block copolymer, named 433BL) and provided comparably good quality, clear prints with minimum satellites or splashes. P[(HEA$_{72}$-*st*-HMAA$_{8}$)-*b*-PMA$_{20}$] (in CF2) also resulted in good, clear prints; it is generally accepted that "typical" drop size and shape can indicate the print quality and performance. However, non-typical drop shapes can also provide good prints as seen with CF2. Formulations containing the highest hydrophobic block length (PPMA$_{40}$, CF3 and CF4) resulted in the poorest prints, as judged by visual inspection.

To ascertain the adhesive properties of the block copolymers in these formulations (CF1 – CF4 *vs.* 433BL), a wider range of hydrophobic substrates were employed; namely PP, PET, high-density polyethylene (HDPE), low-density polyethylene (LDPE) and glass (see Figure 7). Formulations containing P[(HEA_x-*st*-$HMAA_y$)-*b*-PMA_z] block copolymers outperform commercial inks (see Table S12) when printed onto all hydrophobic substrates assessed in this study, where the most promising binding results were between block copolymer formulations and PET. These formulations produced printing comparable to the commercially available ink with legible code and no misplaced drops or obvious defects.

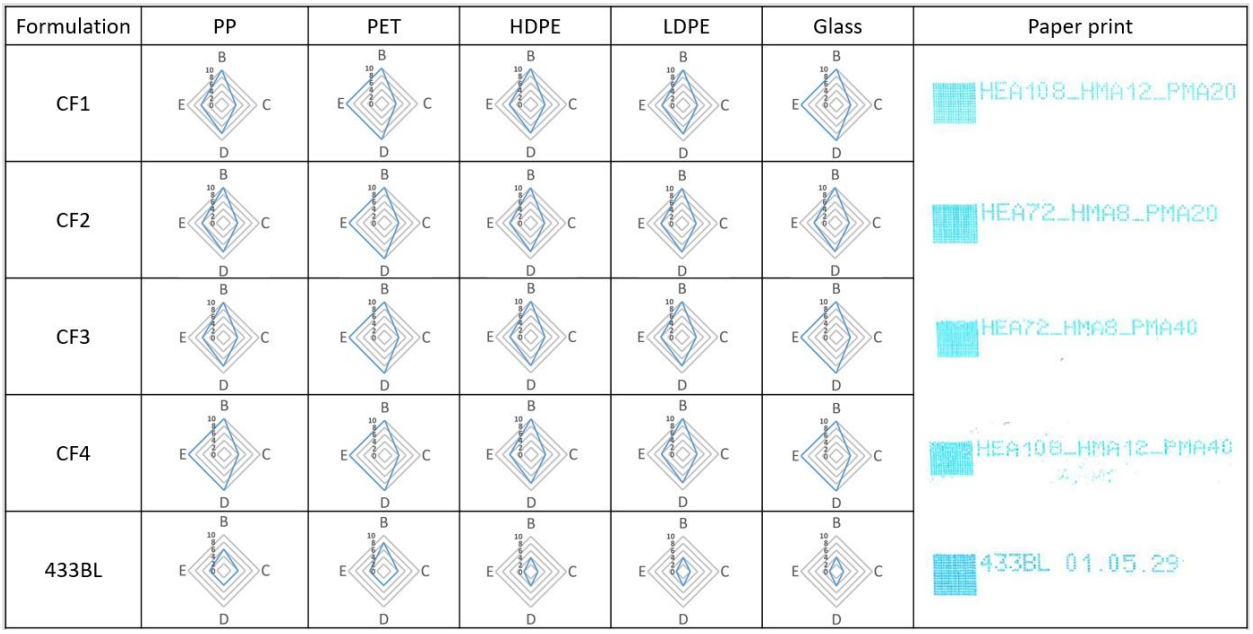

Figure 7. Adhesion tests after printing block copolymer-containing ink formulations (CF1 – CF4) against a commercial formulation (433BL) onto PP, PET, HDPE, LDPE and glass after heating at 150°C for 3 hours. B – finger rub, C – nail scratch, D – tape 610 and E – tape 810.

Conclusions

We have designed and synthesized a range of novel poly[(2-hydroxyethyl acrylate-*stat*-*N*-hydroxymethyl acrylamide)-*block*-propyl methacrylate], P[(HEA-*st*-HMAA)-*b*-PMA], amphiphilic block copolymers with dual functionality. Such polymers were utilized in aqueous-based inkjet printing onto hydrophobic substrates, whereby post-deposition crosslinking and annealing binds the inks to the substrate whilst rendering them insoluble in water. Specifically, two solvents with differing polarities were investigated (DMF and methanol) for the RAFT polymerization, as well as two appropriate CTAs (CPDT and DCMP). This investigation identified scalable methods, which facilitate control over molecular parameters such as M_n, $Đ$, HMAA loading and block ratio, for the synthesis of dual-functional block copolymers. Full control over these parameters enabled manipulation of key performance indicators; namely (i) aqueous dispersion viscosity, (ii) crosslinking time required to render the copolymers insoluble and (iii) adhesive performance on hydrophobic substrates.

Ink formulations that incorporated the dual-functional amphiphilic block copolymers were shown to be successfully printed from aqueous-based formulations to provide comparable quality prints to commercial inks. Additionally, the polymers demonstrated improved adhesive properties in industrially designed tests on a variety of hydrophobic substrates, when compared to ink formulations that did not include the block copolymers. The crosslinked polymers (post-deposition) significantly outperformed the non-crosslinked polymers and present an exciting new technology for the future of commercial inkjet printing on hydrophobic substrates, which is a key step towards cleaner processes in the medical supply and food packaging industries.

References

1 T. Ashley and M. Willis, Emerging Applications for Ink Jet Technology, *NIP Digit. Fabr. Conf.*, 2003, **1**, 116–117.

2 O. A. Basaran, H. Gao and P. P. Bhat, Nonstandard Inkjets, *Annu. Rev. Fluid Mech.*, 2013, **45**, 85–113.

3 Y. Duan, Y. Huo and L. Duan, Preparation of Acrylic Resins Modified with Epoxy Resins and Their Behaviors as Binders of Waterborne Printing Ink on Plastic Film, *Colloids Surfaces A Physicochem. Eng. Asp.*, 2017, **535**, 225–231.

4 Z. Zołek-Tryznowska and J. Izdebska, Flexographic Printing Ink Modified with Hyperbranched Polymers: Boltorn™ P500 and Boltorn™ P1000, *Dye. Pigment.*, 2013, **96**, 602–608.

5 M. Tryznowski, Z. Żołek-Tryznowska and J. Izdebska-Podsiadły, The Wettability Effect of Branched Polyglycerols Used as Performance Additives for Water-Based Printing Inks, *J. Coatings Technol. Res.*, 2018, **15**, 649–655.

6 P. Pi, W. Wang, X. Wen, S. Xu and J. Cheng, Synthesis and Characterization of Low-Temperature Self-Crosslinkable Acrylic Emulsion for PE Film Ink, *Prog. Org. Coatings*, 2015, **81**, 66–71.

7 A. S. Johns and C. D. Bain, Ink-Jet Printing of High-Molecular-Weight Polymers in Oil-in-Water Emulsions, *ACS Appl. Mater. Interfaces*, 2017, **9**, 22918–22926.

8 J. Zhang, X. Li, X. Shi, M. Hua, X. Zhou and X. Wang, Synthesis of Core-Shell Acrylic-Polyurethane Hybrid Latex as Binder of Aqueous Pigment Inks for Digital Inkjet Printing, *Prog. Nat. Sci. Mater. Int.*, 2012, **22**, 71–78.

9 M. Sangermano, A. Chiolerio, G. Marti and P. Martino, UV-Cured Acrylic Conductive Inks for Microelectronic Devices, *Macromol. Mater. Eng.*, 2013, **298**, 607–611.

10 S. Magdassi, *The Chemistry of Inkjet Inks*, 2009.

11 I. M. Hutchings and G. D. Martin, *Inkjet Technology for Digital Fabrication*, 2013.

12 S. Edison, *UV-Curable Inkjet Inks: Revolutionize Industrial Printing*, 2006.

13 J. Chiefari, Y. K. B. Chong, F. Ercole, J. Krstina, J. Jeffery, T. P. T. Le, R. T. A. Mayadunne, G. F. Meijs, C. L. Moad, G. Moad, E. Rizzardo and S. H. Thang, Living Free-Radical Polymerization by Reversible Addition - Fragmentation Chain Transfer : The RAFT Process, *Macromolecules*, 1998, **31**, 5559–5562.

14 G. Moad, E. Rizzardo and S. H. Thang, Living Radical Polymerization by the RAFT Process—A First Update, *Aust. J. Chem.*, 2006, **59**, 669.

15 M. Destarac, C. Brochon, J. M. Catala, A. Wilczewska and S. Z. Zard, Macromolecular Design via the Interchange of Xanthates (MADIX): Polymerization of Styrene with O-ethyl Xanthates as Controlling Agents, *Macromol. Chem. Phys.*, 2002, **203**, 2281–2289.

16 S. Z. Zard, The Genesis of the Reversible Radical Addition-Fragmentation-Transfer of Thiocarbonylthio Derivatives from the Barton-McCombie Deoxygenation: A Brief Account and Some Mechanistic Observations, *Aust. J. Chem.*, 2006, **59**, 663–668.

17 N. Pullan, M. Liu and P. D. Topham, Reversible Addition-Fragmentation Chain Transfer Polymerization of 2-Chloro-1,3-Butadiene, *Polym. Chem.*, 2013, **4**, 2272–2277.

18 A. Isakova, P. D. Topham and A. J. Sutherland, Controlled RAFT Polymerization and Zinc Binding Performance of Catechol-Inspired Homopolymers, *Macromolecules*, 2014, **47**, 2561–2568.

19 I. Fraga Domínguez, J. Kolomanska, P. Johnston, A. Rivaton and P. D. Topham, Controlled Synthesis of Poly(Neopentyl p -Styrene Sulfonate) via Reversible Addition-Fragmentation Chain Transfer Polymerisation, *Polym. Int.*, 2015, **64**, 621–630.

20 J. Kolomanska, P. Johnston, A. Gregori, I. Fraga Domínguez, H.-J. Egelhaaf, S. Perrier, A. Rivaton, C. Dagron-Lartigau and P. D. Topham, Design, Synthesis and Thermal Behaviour of a Series of Well-Defined Clickable and Triggerable Sulfonate Polymers, *RSC Adv.*, 2015, **5**, 66554–66562.

21 C. A. Kuliasha, R. L. Fedderwitz, P. R. Calvo, B. S. Sumerlin and A. B. Brennan, Engineering the Surface Properties of Poly(Dimethylsiloxane) Utilizing Aqueous RAFT Photografting of Acrylate/Methacrylate Monomers, *Macromolecules*, 2018, **51**, 306–317.

22 B. Couturaud, P. G. Georgiou, S. Varlas, J. R. Jones, M. C. Arno, J. C. Foster and R. K. O'Reilly, Poly(Pentafluorophenyl Methacrylate)-Based Nano-Objects Developed by Photo-PISA as Scaffolds for Post-Polymerization Functionalization, *Macromol. Rapid Commun.*, 2019, **40**, 1800460 (1-6).

23 M. R. Hill, R. N. Carmean and B. S. Sumerlin, Expanding the Scope of RAFT Polymerization: Recent Advances and New Horizons, *Macromolecules*, 2015, **48**, 5459–5469.

24 C. A. Figg and B. S. Sumerlin, Aqueous Visible-Light RAFT Polymerizations and Applications. In *Reversible Deactivation Radical Polymerization: Materials and Applications*, USA, 2018, 43–56.

25 R. N. Carmean, T. E. Becker, M. B. Sims and B. S. Sumerlin, Ultra-High Molecular Weights via Aqueous Reversible-Deactivation Radical Polymerization, *Chem*, 2017, **2**, 93–101.

26 H. Sun, C. P. Kabb, M. B. Sims and B. S. Sumerlin, Architecture-Transformable Polymers: Reshaping the Future of Stimuli-Responsive Polymers, *Prog. Polym. Sci.*, 2019, **89**, 61–75.

27 C. D. Vo, J. Rosselgong, S. P. Armes and N. C. Billingham, RAFT Synthesis of Branched Acrylic Copolymers, *Macromolecules*, 2007, **40**, 7119–7125.

28 C. Chen, X. Guo, J. Du, B. Choi, H. Tang, A. Feng and S. H. Thang, Synthesis of Multifunctional Miktoarm Star Polymers *via* an RGD Peptide-Based RAFT Agent, *Polym. Chem.*, 2019, **10**, 228–234.

29 N. J. Warren and S. P. Armes, Polymerization-Induced Self-Assembly of Block Copolymer Nano-Objects via RAFT Aqueous Dispersion Polymerization, *J. Am. Chem. Soc.*, 2014, **136**, 10174–10185.

30 M. Destarac, Industrial Development of Reversible-Deactivation Radical Polymerization: Is the Induction Period Over?, *Polym. Chem.*, 2018, **9**, 4947–4967.

31 L. J. Chen, W. U. Feng, D. S. Li, Y. Jian and R. X. Li, Preparation of Self-Crosslinked Acrylate Emulsion with High Elasticity and Its Rheological Properties, *J. Cent. South Univ. Technol*, 2008, **15**, 324–328.

32 Z. Coe, A. Weems, A. P. Dove and R. K. O'Reilly, Synthesis of Monodisperse Cylindrical Nanoparticles via Crystallization-driven Self-assembly of Biodegradable Block Copolymers, *J. Vis. Exp.*, DOI:10.3791/59772.

33 M. Alauhdin, T. M. Bennett, G. He, S. P. Bassett, G. Portale, W. Bras, D. Hermida-Merino and S. M. Howdle, Monitoring Morphology Evolution within Block Copolymer Microparticles during Dispersion Polymerisation in Supercritical Carbon Dioxide: A High Pressure SAXS Study, *Polym. Chem.*, 2019, **10**, 860–871.

34 C. György, J. R. Lovett, N. J. W. Penfold and S. P. Armes, Epoxy-Functional Sterically Stabilized Diblock Copolymer Nanoparticles via RAFT Aqueous Emulsion Polymerization: Comparison of Two Synthetic Strategies, *Macromol. Rapid Commun.*, 2019, **40**, 1–7.

35 M. Douverne, Y. Ning, A. Tatani, F. C. Meldrum and S. P. Armes, How Many Phosphoric Acid Units Are Required to Ensure Uniform Occlusion of Sterically Stabilized Nanoparticles within Calcite?, *Angew. Chemie - Int. Ed.*, 2019, **58**, 8692–8697.

36 M. Guerre, S. M. W. Rahaman, B. Améduri, R. Poli and V. Ladmiral, Limits of Vinylidene Fluoride RAFT Polymerization, *Macromolecules*, 2016, **49**, 5386–5396.

37 G. Moad, Y. K. Chong, A. Postma, E. Rizzardo and S. H. Thang, Advances in RAFT Polymerization: The Synthesis of Polymers with Defined End-Groups, *Polymer (Guildf).*, 2005, **46**, 8458–8468.

38 S. Perrier, 50th Anniversary Perspective: RAFT Polymerization - A User Guide, *Macromolecules*, 2017, **50**, 7433–7447.

39 M. Benaglia, J. Chiefari, Y. K. Chong, G. Moad, E. Rizzardo and S. H. Thang, Universal (Switchable) RAFT Agents, *J. Am. Chem. Soc.*, 2009, **131**, 6914–6915.

40 W. Steinhauer, R. Hoogenboom, H. Keul and M. Moeller, Copolymerization of 2-Hydroxyethyl Acrylate and 2-Methoxyethyl Acrylate via RAFT: Kinetics and Thermoresponsive Properties, *Macromolecules*, 2010, **43**, 7041–7047.

41 W. Steinhauer, R. Hoogenboom, H. Keul and M. Moeller, Block and Gradient Copolymers of 2-Hydroxyethyl Acrylate and 2-Methoxyethyl Acrylate via RAFT: Polymerization Kinetics, Thermoresponsive Properties and Micellization, *Macromolecules*, 2013, **46**, 1447–1460.

42 D. E. Discher and A. Eisenberg, Polymer Vesicles, *Science*, 2002, **297**, 967–973.

43 L. Zhang and A. Eisenberg, Multiple Morphologies of 'Crew-Cut' Aggregates of Polystyrene-b-Poly(Acrylic Acid) Block Copolymers, *Science,* 1995, **268**, 1728–1731.

44 Y. Y. Won, H. Ted Davis and F. S. Bates, Giant Wormlike Rubber Micelles, *Science*, 1999, **283**, 960–963.

45 J. N. Israelachvili, D. J. Mitchell and B. W. Ninham, Theory of Self-Assembly of Hydrocarbon Amphiphiles into Micelles and Bilayers, *J. Chem. Soc. Faraday Trans. 2 Mol. Chem. Phys.*, 1976, **72**, 1525–1568.

46 S. Förster and M. Antonietti, Amphiphilic Block Copolymers in Structure-Controlled Nanomaterial Hybrids, *Adv. Mater.*, 1998, **10**, 195–217.

47 M. Antonietti and S. Förster, Vesicles and Liposomes: A Self-Assembly Principle Beyond Lipids, *Adv. Mater.*, 2003, **15**, 1323–1333.

48 B. M. Discher, Y. Y. Won, D. S. Ege, J. C. M. Lee, F. S. Bates, D. E. Discher and D. A. Hammer, Polymersomes: Tough Vesicles Made from Diblock Copolymers, *Science*, 1999, **284**, 1143–1146.

49 A. Blanazs, J. Madsen, G. Battaglia, A. J. Ryan and S. P. Armes, Mechanistic Insights for Block Copolymer Morphologies : How Do Worms Form Vesicles ?, *J. Am. Chem. Soc.*, 2011, **133**, 16581–16587.

50 A. J. Parnell, N. Tzokova, P. D. Topham, D. J. Adams, S. Adams, C. M. Fernyhough, A. J. Ryan and R. A. L. Jones, The Efficiency of Encapsulation within Surface Rehydrated Polymersomes, *Faraday Discuss.*, 2009, **143**, 29–46.

51 G. Tillet, B. Boutevin and B. Ameduri, Chemical Reactions of Polymer Crosslinking and Post-Crosslinking at Room and Medium Temperature, *Prog. Polym. Sci.*, 2011, **36**, 191–217.

52 H. Willcock and R. K. O'Reilly, End Group Removal and Modification of RAFT Polymers, *Polym. Chem.*, 2010, **1**, 149–157.

53 D. J. Keddie, G. Moad, E. Rizzardo and S. H. Thang, RAFT Agent Design and Synthesis, *Macromolecules*, 2012, **45**, 5321–5342.

54 D. J. Keddie, A Guide to the Synthesis of Block Copolymers Using Reversible-Addition Fragmentation Chain Transfer (RAFT) Polymerization, *Chem. Soc. Rev.*, 2014, **43**, 496–505.

55 P. L. Dubin, S. Koontz and K. L. Wright, Substrate-Polymer Interactions in Liquid Exclusion Chromatography (GPC) in N,N-Dimethylformamide, *J. Polym. Sci.*, 1977, **15**, 2047–2057.

56 J. Zhang, R. Deubler, M. Hartlieb, L. Martin, J. Tanaka, E. Patyukova, P. D. Topham, F. H. Schacher and S. Perrier, Evolution of Microphase Separation with Variations of Segments of Sequence-Controlled Multiblock Copolymers, *Macromolecules*, 2017, **50**, 7380-7387.

57 A. Gescher, Metabolism of N,N-Dimethylformamide: Key to the Understanding of Its Toxicity, *Chem. Res. Toxicol.*, 1993, **6**, 245–251.

58 C. P. Jesson, V. J. Cunningham, M. J. Smallridge and S. P. Armes, Synthesis of High Molecular Weight Poly(Glycerol Monomethacrylate) via RAFT Emulsion Polymerization of Isopropylideneglycerol Methacrylatefree, *Macromolecules*, 2018, **51**, 3221–3232.

59 V. J. Cunningham, A. M. Alswieleh, K. L. Thompson, M. Williams, G. J. Leggett, S. P. Armes, B. Hill, S. Y. S and O. M. Musa, Poly(Glycerol Monomethacrylate) − Poly(benzyl Methacrylate) Diblock Copolymer Nanoparticles via RAFT Emulsion Polymerization: Synthesis, Characterization, and Interfacial Activity, *Macromolecules*, 2014, **47**, 5613–5623.

60 H. R. Brown, Adhesion Between Polymers and Other Substances - A Review of Bonding Mechanisms, Systems and Testing, *Mater. Forum*, 2000, **24**, 49–58.

61 S. S. Voyutskii and V. L. Vakula, The Role of Diffusion Phenomena in Polymer-to-Polymer Adhesion, *J. Appl. Polym. Sci.*, 1963, **7**, 475–491.

62 B. Derby, Inkjet Printing of Functional and Structural Materials: Fluid Property Requirements, Feature Stability and Resolution, *Annu. Rev. Mater. Res.*, 2010, **40**, 395–414.

63 C.-D. Vo, J. Rosselgong, S. P. Armes and N. Tirelli, Stimulus-Responsive Polymers Based on 2-Hydroxypropyl Acrylate Prepared by RAFT Polymerization, *J. Polym. Sci. Part A Polym. Chem.*, 2010, **48**, 2032–2043.

For Table of Contents Use Only

Thermally Triggerable, Anchoring Block Copolymers for use in Aqueous Inkjet Printing

George E. Parkes, Helena J. Hutchins-Crawford, Claire Bourdin, Stuart Reynolds, Laura Leslie, Matthew J. Derry, Josephine L Harries, Paul D. Topham